JPET Fast Forward. Published on June 2, 2009 as DOI: 10.1124/jpet.109.154781

JPET # 154781

P-glycoprotein and Breast Cancer Resistance Protein

Influence Brain Distribution of Dasatinib

Ying Chen, Sagar Agarwal, Naveed M. Shaik, Cliff Chen, Zheng Yang, William F. Elmquist

Department of Pharmaceutics, University of Minnesota, Minneapolis, MN, U.S.A. (Y.C., S.A., N.M.S. and W.F.E.)

Metabolism and Pharmacokinetics, Pharmaceutical Candidate Optimization, Bristol-Myers Squibb Co., Princeton, NJ, USA (C.C. and Z.Y.)

JPET Fast Forward. Published on June 2, 2009 as DOI: 10.1124/jpet.109.154781
This article has not been copyedited and formatted. The final version may differ from this version.

Running Title:

Active efflux limits CNS distribution of dasatinib

Corresponding Author

William F. Elmquist, Department of Pharmaceutics, University of Minnesota, 9-177 Weaver Densford Hall, 308 Harvard Street SE, Minneapolis, MN 55455, USA. Phone: +001-612-625-0097; Fax: +001-612-626-2125; e-mail: elmqu011@umn.edu

Number of text pages – 16

Number of figures – 6

Number of tables – 2

Number of references – 29

Number of words in abstract – 243

Number of words in introduction – 593

Number of words in discussion – 1464

List of Abbreviations

CML, Chronic myelogenous leukemia; Ph, philadelphia chromosome; ALL, acute lymphoblastic leukemia; CNS, central nervous system; BBB, blood-brain-barrier; Mdr1, multi-drug resistance protein 1; P-gp, p-glycoprotein; BCRP, breast cancer resistance protein; BCR, breakpoint cluster region; ABL, Abelson; PDGFR, platelet-derived growth factor; TKI, tyrosine kinase inhibitors; A-to-B, apical-to-basolateral; B-to-A, basolateral-to-apical; P_{eff}, effective permeability; B/P , brain-to-plasma; ER, efflux ratio; GBM , glioblastoma multiforme.

JPET Fast Forward. Published on June 2, 2009 as DOI: 10.1124/jpet.109.154781
This article has not been copyedited and formatted. The final version may differ from this version.

Abstract

The novel tyrosine kinase inhibitor dasatinib is approved for use in imatinib resistant or intolerant chronic myelogenous leukemia (CML) and may be useful for other tumors in the CNS. The objective of this study was to investigate the role of p-glycoprotein (P-gp) and breast cancer resistance protein (BCRP) in modulating the CNS penetration of dasatinib. Results from the *in vitro* studies indicate that cellular delivery of dasatinib is significantly limited by active efflux due to both P-gp and BCRP. Permeability studies indicated greater permeability in the basolateral-to-apical direction than in the apical-to-basolateral direction due to active efflux by P-gp or BCRP. Selective inhibitors of P-gp and BCRP, such as LY335979 and Ko143, were able to restore the intracellular accumulation and abolish the directionality in net flux of dasatinib. *In vivo* brain distribution studies showed that the CNS distribution of dasatinib is limited with the brain-to-plasma concentration ratios less than 0.12 in wild-type mice, which increased approximately 8-fold in *Mdr1a/b*$^{-/-}$ *Bcrp1*$^{-/-}$ mice. Dasatinib brain distribution was significantly increased in *Mdr1a/b*$^{-/-}$ mice and when wild-type mice were pretreated with LY335979. Simultaneous inhibition of P-gp and BCRP by GF120918 resulted in a 5-fold increase in brain concentration. These *in vitro* and *in vivo* studies demonstrate that dasatinib is a substrate for the important efflux transporters p-glycoprotein and BCRP. These transport systems play a significant role in limiting the CNS delivery of dasatinib and may have direct implications in the treatment of primary and metastatic brain tumors.

JPET Fast Forward. Published on June 2, 2009 as DOI: 10.1124/jpet.109.154781
This article has not been copyedited and formatted. The final version may differ from this version.

Chronic myelogenous leukemia (CML) accounts for 15-20% of all cases of adult leukemia in western populations (Quintas-Cardama et al., 2007). Imatinib (*Gleevec, STI 571*) is a first-generation tyrosine kinase inhibitor (TKI) that was approved for use in the treatment of CML and gastrointestinal stromal tumor (GIST) (Druker, 2003a). Imatinib inhibits the BCR-ABL, c-kit, platelet-derived growth factor (PDGFR) and the ARG tyrosine kinases (Druker, 2003b). CNS involvement is a common complication seen in CML and most patients with CML and Ph^+ acute lyphoblastic leukemia (Ph^+ ALL) develop extramedullary involvement during the course of their disease. CNS failure has been reported in approximately 20% of imatinib-treated patients with CML or Ph^+ ALL (Leis et al., 2004). CNS relapses were observed in patients despite a complete hematological response (Leis et al., 2004). This can be attributed to the poor penetration of imatinib across the blood-brain barrier (BBB) resulting in sub-therapeutic drug levels in the brain. This limited delivery of imatinib to the brain is primarily a result of active efflux at the BBB by drug eluting P-glycoprotein (P-gp) and the breast cancer resistance protein (BCRP). Our laboratory and several others have reported that imatinib is a good substrate for these two drug transporters which limit CNS distribution (Dai et al., 2003; Breedveld et al., 2005). An inadequate concentration of imatinib in the CNS can make the brain a sanctuary for chronic myelogenous leukemia (Leis et al., 2004; Neville et al., 2004; Rajappa et al., 2004).

Dasatinib (*Sprycel;BMS-354825*) is a second-generation TKI approved for use in imatinib-resistant CML patients (Shah, 2007). Dasatinib is an extremely potent BCR-ABL inhibitor and has shown significant activity in imatinib-resistant or intolerant CML patients (Cortes et al., 2007; Kantarjian et al., 2007; Ottmann et al., 2007). It effectively inhibits the proliferation of tumor cells expressing nearly all imatinib-resistant isoforms of BCR-ABL (2006). In addition to this, dasatinib also inhibits the SRC tyrosine kinase (Lombardo et al., 2004) which has been identified as a potential target for glioblastoma therapy (Du et al., 2009). Given that dasatinib was designed to overcome the molecular resistance seen with imatinib, one question that arises is whether dasatinib can also overcome the CNS delivery problem and prevent CNS metastasis. There is little information available about the delivery of dasatinib across the BBB, including the action of relevant BBB transporters in modulating this delivery. As a promising multi-targeted TKI, adequate CNS delivery of dasatinib is important for the prevention of CNS metastases in CML as well as treatment of other CNS malignancies.

It was recently suggested that dasatinib can cross the BBB to achieve therapeutic response in a mouse model of CML and in Ph(+) ALL and CML patients with CNS involvement (Porkka et al., 2008). However, dasatinib brain concentrations were on average 12- to 31-fold lower than the plasma concentrations and the therapeutic benefit was attributed to the extremely high potency of dasatinib against the BCR-ABL and SRC therapeutic targets. The fact that this low level of brain penetrance was able to result in anti-tumor activity may be true in this case, but may not hold for other tumors of the CNS, such as those driven by less sensitive tyrosine kinase targets, e.g., c-kit. In general, the limited CNS distribution of dasatinib may be a consideration in developing new therapeutic strategies for the treatment of brain tumors. Therefore, the objective of this study was to investigate the extent to which dasatinib can distribute to the brain and to establish the influence of active efflux by P-gp and BCRP at the blood-brain barrier on the brain distribution of dasatinib.

JPET Fast Forward. Published on June 2, 2009 as DOI: 10.1124/jpet.109.154781
This article has not been copyedited and formatted. The final version may differ from this version.

Methods

Chemicals and Reagents

Dasatinib and [^{14}C]-dasatinib (31.9 µCi/mg) were kindly provided by Bristol-Myers Squibb Company (Princeton, NJ). [^{3}H]-vinblastine sulfate and [^{3}H]-mitoxantrone were purchased from Moravek Biochemicals (La Brea, CA). LY335979 (zosuquidar, (*R*)-4-((1a*R*,6*R*,10b*S*)-1,2-difluoro-1,1a,6,10b-tetrahydrodibenzo-(*a*,*e*)cyclopropa(*c*) cycloheptan-6-yl)-α-((5-quinoloyloxy)methyl)-1-piperazineethanol, trihydrochloride) was a gift from Eli Lilly and Co. (Indianapolis, IN), GF120918 (elacridar, N-[4-[2-(6, 7-Dimethoxy-3, 4-dihydro-1H-isoquinolin-2-yl) ethyl]-5-methoxy-9-oxo-10H-acridine-4-carboxamide) was generously given by GlaxoSmithKline (Research Triangle, NC). Dr. Alfred H. Schinkel (The Netherlands Cancer Institute, Amsterdam, The Netherlands) kindly provided Ko143 (Allen et al., 2002). Cell culture reagents were purchased from Invitrogen (Carlsbad, CA). All other reagents and chemicals were purchased from Sigma-Aldrich (St. Louis, MO).

In vitro studies - Cell lines

Epithelial Madine Darby Canine Kidney (MDCKII) cells were used in all *in vitro* studies. Wild-type (WT) and MDR1-transfected cells were a gift from Dr. Piet Borst (Netherlands Cancer Institute), and WT and Bcrp1-transfected cells were kindly provided by Dr. Alfred H. Schinkel (The Netherlands Cancer Institute, Amsterdam, The Netherlands). Cells were cultured in DMEM media supplemented with 10% fetal bovine serum (SeraCare Life Sciences, Inc., Oceanside, CA), penicillin (100 U/ml), streptomycin (100 µg/ml) and amphotericin B 250ng/mL (Sigma-Aldrich, St. Louis, MO) and maintained at 37°C with 5% CO_2 under humidifying conditions. Cells between passages 5 and 15 were used in all experiments.

Intracellular Accumulation Studies in MDCKII Cells

The wild-type and MDR1- or Bcrp1-transfected cells were seeded in clear polystyrene 12-well plates (TPP cell culture plate; Sigma-Aldrich, St. Louis, MO) at a seeding density of 2×10^5 cells/well. The medium was changed on alternate days until the cells formed confluent monolayers. On the day of the experiment, the medium was aspirated and the monolayer was washed twice with 1 mL prewarmed (37°C) assay buffer. The cells were preincubated with 1 ml

JPET Fast Forward. Published on June 2, 2009 as DOI: 10.1124/jpet.109.154781
This article has not been copyedited and formatted. The final version may differ from this version.

of assay buffer for 30 min, after which the buffer was aspirated and the experiment was initiated by adding tracer solution of radiolabeled drug (1 μg [^{14}C] dasatinib, or tracer vinblastine or mitoxantrone for positive controls) in 1 ml assay buffer per well. The plates were continuously agitated at 60 rpm in an orbital shaker maintained at 37°C for the duration of the experiment. At the end of the 3-hour accumulation period, the assay buffer containing the radiolabeled drug was aspirated from all the wells and the cells were washed three times with 2 ml of ice-cold phosphate-buffered saline. Cells were then solubilized using 1 ml of mammalian protein extraction reagent (M-PER®, Pierce Biotechnology, Inc., Rockford, IL). A 200 μl sample of solubilized cell fractions was drawn from each well in triplicate, 4 ml of scintillation fluid (ScintiSafe Econo cocktail; Fisher Scientific Co., Pittsburgh, PA) was added to each sample and counted using liquid scintillation counting (LS-6500; Beckman Coulter, Inc., Fullerton, CA) to determine the radioactivity associated with the cell fractions. The protein concentration was determined using the BCA protein assay (Pierce Biotechnology, Inc., Rockford, IL) to normalize the radioactivity in each well for cell number. For inhibition studies, the cells were treated with the selective inhibitors 1 μM LY335979 for P-gp and 200 nM Ko143 for BCRP during both the preincubation and the accumulation periods. Drug accumulation in cells was expressed as a percentage of the accumulated radioactivity measured in the wild-type control cells (dpm) per microgram of protein. The stock solutions for all the inhibitors used were prepared in dimethyl sulfoxide (DMSO) and diluted using assay buffer to obtain working solutions, so that the final concentration of DMSO was less than 0.1%.

Directional Flux across MDCKII Monolayers

The methods used for directional flux were similar to that previously described by Dai et al. (Dai et al., 2003). Briefly, cells were seeded at a density of 2×10^5 cells/well on polyester semipermeable membrane supports of the inserts in six-well transwells (Corning Inc., Corning, NY). The medium was changed on alternate days and the cells formed confluent polarized epithelial monolayers in 3-4 days. The representative transepithelial electrical resistance was 300 ± 8 ohm·cm^2 (n=6) in the WT MDCKII monolayers, 275 ± 26 ohm·cm^2 (n=6) in the MDR1-transfected MDCKII monolayers and 248± 27 ohm·cm^2 (n=6) in the Bcrp1-transfected MDCKII

JPET Fast Forward. Published on June 2, 2009 as DOI: 10.1124/jpet.109.154781
This article has not been copyedited and formatted. The final version may differ from this version.

monolayers. Mannitol flux across the monolayer was also measured to confirm the existence of tight junctions with approximately 1% per hour flux ($P_{eff} = 9 \times 10^{-8}$ cm/s). The monolayers were washed with 2 mL prewarmed (37°C) assay buffer, and after a 30-min preincubation period, the experiment was initiated by adding a tracer solution of radiolabeled drug (1.5 μg or 2.6 μg ^{14}C-dasatinib) in assay buffer to the donor side (apical side, 1.5 ml; basolateral side, 2.6 ml). Fresh assay buffer was added to the receiver side and 200 μl was sampled from the receiver compartment at 0, 10, 20, 30, 45, 60, and 90 min. The volume sampled was immediately replaced with fresh assay buffer. Additional samples were drawn at 0 and 90 min from the donor compartment. The amount of radioactivity in the samples was determined using liquid scintillation counting. The apical-to-basolateral (A-to-B) flux was determined by addition of radiolabeled drug solution to the apical compartment and sampling the basolateral compartment, whereas for basolateral-to-apical (B-to-A) flux, the donor was the basolateral compartment and the apical compartment was sampled at the mentioned times. When an inhibitor was used in the flux study, the cell monolayers were preincubated with the inhibitor (1 μM LY335979 for P-gp and 200 nM Ko143 for Bcrp1) for 30 min, followed by determination of A-to-B and B-to-A flux with the inhibitor being present in both compartments throughout the course of the experiment.

Permeability Calculation

The effective permeability (*P*eff) was calculated by the following equation,

$$P_{eff} = \frac{\left(\frac{dQ}{dt}\right)}{A * C_0}$$

where *Q* is the amount of radiolabeled drug transported though the cell monolayer, t is time, *dQ/dt* is the mass transport rate, *A* is the apparent surface area of the cell monolayer (4.67 cm^2), and C_0 is the initial donor concentration. The efflux ratio (ER) is defined as the ratio of P_{eff} in the B-to-A direction to the P_{eff} in the A-to-B direction and gives an indication of the magnitude of P-gp or Bcrp1 mediated efflux.

***In vivo* studies**

Animals

JPET Fast Forward. Published on June 2, 2009 as DOI: 10.1124/jpet.109.154781
This article has not been copyedited and formatted. The final version may differ from this version.

Animals used in this study were male *Mdr1a/b*$^{-/-}$ (P-gp knockout), *Bcrp1*$^{-/-}$ (Bcrp1 knockout), *Mdr1a/b*$^{-/-}$ *Bcrp1*$^{-/-}$ (triple knockout) and wild-type mice of a FVB genetic background. All mice were purchased from Taconic Farms. Inc. (Germantown, NY) and were between 8 to 10 weeks old at the time of experiment. Animals were maintained under temperature-controlled conditions with a 12-h light/dark cycle and unlimited access to food and water. All mice were allowed to acclimatize for a minimum of one week upon arrival. All studies were approved by the Institutional Animal Care and Use Committee of the University of Minnesota (IACUC).

Dasatinib Brain and Plasma Distribution Studies in Mice.

All mice received dasatinib (1:1 propylene glycol: water, pH 4.6) by intravenous administration in the tail vein at a dose of 5 mg/kg or an oral dose of 10 mg/kg. The study involved the following five study groups.

(i) Wild-type and *Mdr1a/b*$^{-/-}$ *Bcrp1*$^{-/-}$ mice received i.v. dasatinib following which blood and brain were sampled at 5, 20, 60, 120, 180 min postdose, n=4 at each time point.

(ii) Wild-type mice received 25 mg/kg LY335979, 10 mg/kg Ko143 or 10 mg/kg GF120918 intravenously 30 minutes before i.v. dasatinib, and brain and blood were sampled at 20 and 120 minutes, n=4 at each time point.

(iii) Wild-type, *Mdr1a/b*$^{-/-}$, *Bcrp1*$^{-/-}$, *Mdr1a/b*$^{-/-}$ *Bcrp1*$^{-/-}$ mice were administered i.v. dasatinib, blood and brain were sampled at 20 and 120 minutes post-dose, n=4 at each time point.

(iv) Wild-type mice received 25 mg/kg LY335979, 10 mg/kg Ko143 or 10 mg/kg GF120918 intravenously 30 minutes before an oral dose of dasatinib, brain and blood were sampled at 120 minutes, n=4.

(v) Wild-type, *Mdr1a/b*$^{-/-}$, *Bcrp1*$^{-/-}$, *Mdr1a/b*$^{-/-}$ *Bcrp1*$^{-/-}$ mice were administered dasatinib by oral gavage, blood and brain were sampled at 120 minutes post-dose, n=4.

The animals were euthanized at predetermined time points by using a CO_2 chamber. Blood was immediately harvested via cardiac puncture and collected in tubes preloaded with potassium EDTA (BD, Franklin Lakes, NJ). Whole brain was immediately harvested, rinsed with ice-cold saline to remove extraneous blood and flash frozen using liquid nitrogen. Plasma was isolated from blood by centrifugation at 3000 rpm for 10 min at 4°C. All plasma and whole brain samples were stored at -80°C until analysis by LC-MS/MS.

Determination of Dasatinib Concentrations in Plasma and Brain using LC-MS/MS

Mouse plasma and brain samples were analyzed by LC-MS/MS. Sample preparation included addition of 3 volumes of acetonitrile containing internal standard (IS) d6-dasatinib to the plasma samples. Whole brain samples were first homogenized in water with a volume ratio of 1:3 followed by the addition of acetonitrile containing IS. After centrifugation to remove precipitated proteins, 10 µL of the clear supernatant was analyzed by LC/MS/MS. Chromatographic separation was obtained using an Atlantis® dC18 column (2.1 mm x 50 mm) packed with a 3µM stationary phase (Waters Corporation, Milford, MA). The mobile phase was composed of 10 mM ammonium acetate with 0.1% formic acid (A) and acetonitrile (B). A gradient elution method was used with the initial mobile phase consisting of 90% A and 10% B. After sample injection, the mobile phase was held at the initial condition for 1 min and then changed to 10% solvent A and 90% solvent B over 1 min and held at that composition for an additional 0.8 minutes. The mobile phase was then returned to initial conditions and the column was re-equilibrated for one minute. The total analysis time was 4 minutes. The HPLC was interfaced to a Micromass Quattro LC triple quadrupole mass spectrometer (Waters, Milford, MA, USA) equipped with electrospray ionization interface. The desolvation temperature was 350°C and the source temperature was 120°C. Data acquisition employed selected reaction monitoring (SRM). Positively charged ions representing the $[MH]^+$ for dasatinib and the internal standard (IS) were selected in MS1 and dissociated with argon at a pressure of 2.5×10^{-3} Torr to form specific product ions which were subsequently monitored by MS2. All dwell times were 100 ms. The SRM transitions monitored were m/z 488 → 401 for dasatinib, m/z 496 → 409 for the internal standard. The cone voltage was optimized at 35 V for both dasatinib and IS, while the collision energy was 35 eV. The retention time for dasatinib and IS was 2.05 and 2.04 min, respectively. The lower limit of quantification was 1 ng/mL.

Statistical Analysis

Statistical analysis was conducted using SigmaStat, version 3.1(Systat Software, Inc., Point Richmond, CA). Statistical comparisons between two groups were made by using two-sample t-test at $p < 0.01$ significance level. If groups failed the normality test, then the nonparametric alternative of two-sample *t* test, the Mann-Whitney rank sum test was used. Multiple groups were compared by one-way analysis of variance with the Holm-Sidak post-hoc test for multiple

JPET Fast Forward. Published on June 2, 2009 as DOI: 10.1124/jpet.109.154781
This article has not been copyedited and formatted. The final version may differ from this version.

comparisons at a significance level of $p < 0.01$. When groups failed the normality test, the Kruskal-Wallis one way analysis of variance on ranks was used.

Results

Intracellular Accumulation Studies in MDCKII Cells

Intracellular accumulation of [^{14}C] dasatinib was studied in MDCKII-Bcrp1, MDCKII-MDR1 and MDCKII wild-type cells. [^{3}H] Vinblastine, a prototypical P-gp substrate, was included as a positive control in all accumulation studies done in MDR1-transfected cells and showed significantly lower accumulation in the MDR1-transfected cells compared with wild-type cells (~13% of WT control, $p < 0.01$) **(Figure 1).** Similar to the positive control, accumulation of [^{14}C] dasatinib in the MDR1-transfected cells was significantly lower than that in the wild-type cells (~ 15% of WT control, $p < 0.01$). Treatment with 1 μM LY335979, the P-gp selective inhibitor, completely abolished P-gp efflux activity such that there was no significant difference in the accumulation of [^{14}C] dasatinib between the two cell types **(Figure 1)**. Accumulation of dasatinib in the Bcrp1-transfected cells was about 25-fold lower than the accumulation in wild-type cells ($p<0.01$), similar to the positive control for BCRP, mitoxantrone. Use of the BCRP selective inhibitor Ko143 completely abolished this difference in dasatinib accumulation between the Bcrp1-transfected and wild-type cells **(Figure 2).**

Directional Flux across MDCKII Cell Monolayers

Transport of [^{14}C]-dasatinib was studied in MDCKII cells and the effective permeabilities were calculated. In the MDCKII wild-type cells, effective permeability of dasatinib was significantly greater in the B-to-A direction than in the A-to-B direction, yielding an efflux ratio (ER) of 4.8. Similarly, in the MDR1-transfected cells, the effective permeability was significantly enhanced in the B-to-A direction compared to the A-to-B direction with an ER of 25.6. Treatment with 1 μM LY335979 completely abolished this directionality in dasatinib transport by P-gp, such that there was no significant difference in permeabilities of dasatinib in the two directions in either cell type. Use of 1 μM LY335979 dramatically reduced the ER to 0.9 in the wild-type cells and 1.2 in the MDR1-transfected cells **(Table 1A)**. Transport of [^{14}C] dasatinib in the wild-type and Bcrp1-transfected cells also showed significant directionality with the effective permeability significantly increased in the B-to-A direction in both cell types. The ER was 51.5 in the Bcrp1-

transfected cells compared to 4.1 in the wild-type cells. The BCRP inhibitor Ko143 (200nM) was not able to completely abolish this directionality in transport. Permeability of dasatinib in the B-to-A direction decreased resulting in a reduction of the ER to approximately 9 in the Bcrp1-transfected cells compared to 4.1 in the wild-type **(Table 1B)**.

Dasatinib Brain Distribution in Mice

Brain distribution of dasatinib after an i.v. dose was determined in wild-type and *Mdr1a/b*$^{-/-}$ *Bcrp1*$^{-/-}$ mice. There was no significant difference in plasma concentrations between the wild-type and *Mdr1a/b*$^{-/-}$ *Bcrp1*$^{-/-}$ mice **(Figure 3A)**, however, brain concentrations in the *Mdr1a/b*$^{-/-}$ *Bcrp1*$^{-/-}$ triple-knockout mice were significantly greater ($p<0.001$) than that in wild-type mice **(Figure 3B).** The brain-to-plasma concentration ratio (B/P), a measure of the brain distribution, was significantly greater ($p<0.001$) in the triple-knockout mice at all of the five measured time points **(Figure 4)**. The B/P concentration ratio was lower than 0.12 in the wild-type mice at all the time points, suggesting that less than 12% of dasatinib in blood crosses the blood-brain barrier to reach brain. In the triple knockout mice this ratio reached an "equilibrium" value of 1 after 60 mins.

The brain concentrations of dasatinib were also measured in wild-type mice that were pretreated with the efflux inhibitors LY335979, Ko143 or GF120918. P-gp inhibition by LY335979 significantly increased brain dasatinib concentrations in the wild-type mice ($p<0.01$) **(Figure 5A)**. Pretreatment with the BCRP inhibitor Ko143 was not able to increase brain distribution of dasatinib to any significant extent. Interestingly, simultaneous inhibition of both P-gp and BCRP by the dual inhibitor GF120918 resulted in a dramatic increase in brain dasatinib concentrations, the B/P ratio increasing by more than 5-fold at both time points ($p<0.001$). A study was then conducted in wild-type, *Mdr1a/b*$^{-/-}$, *Bcrp1*$^{-/-}$ and *Mdr1a/b*$^{-/-}$ *Bcrp1*$^{-/-}$ to replicate pharmacological inhibition with genetic deletion of drug efflux proteins. Results from this study were similar to those seen when P-gp, BCRP, or P-gp and BCRP were inhibited using pharmacological inhibitors (**Figure 5B**). Brain dasatinib concentrations increased significantly in *Mdr1a/b*$^{-/-}$ mice compared with those in wild-type mice ($p<0.001$). While brain concentrations in *Bcrp1*$^{-/-}$ mice did not increase to any significant extent, brain dasatinib concentrations increased by greater than 10-fold in the *Mdr1a/b*$^{-/-}$ *Bcrp1*$^{-/-}$ mice ($p<0.001$).

JPET Fast Forward. Published on June 2, 2009 as DOI: 10.1124/jpet.109.154781
This article has not been copyedited and formatted. The final version may differ from this version.

Dasatinib brain distribution was also studied after oral administration of drug in FVB mice. Brain concentrations after a 10 mg/kg oral dose of dasatinib were significantly lower than the plasma concentrations. Similar to the intravenous study, brain distribution was enhanced when FVB wild-type mice were treated with efflux inhibitors LY335979, Ko143 or GF120918 prior to receiving oral dasatinib. The brain-to-plasma ratio increased 2-fold on treatment with the P-gp inhibitor, though this difference did not reach significance. Treatment with Ko143 did not change the B/P ratio, however GF120198 dramatically increased the B/P ratio by over 6-fold ($p<0.01$) (**Figure 6**). In the gene knockout animals, the B/P concentration ratio increased approximately 4-fold in the *Mdr1a/b*$^{-/-}$ mice and by over 9-fold in the *Mdr1a/b*$^{-/-}$ *Bcrp1*$^{-/-}$ mice ($p<0.01$). The brain-to-plasma concentration ratio did not change in the *Bcrp1*$^{-/-}$ mice (**Figure 6**).

Discussion

Imatinib mesylate showed initial remarkable efficacy in patients with CML (Druker et al., 2001a; Druker et al., 2001b). However, this success was relatively short-lived with reports of rapid relapse and CNS metastases in imatinib treated patients (Ottmann et al., 2002; Sawyers et al., 2002). This led to the development of dasatinib – an extremely potent inhibitor of the BCR-ABL tyrosine kinase, for use in imatinib resistant and intolerant CML patients. In addition to its potent inhibitory effects against BCR-ABL, dasatinib also inhibits the SRC family proteins (Lombardo et al., 2004; Nam et al., 2005), which have been implicated in the development of resistance and the extramedullary expansion of disease in CML (Donato et al., 2003; Dai et al., 2004; Ptasznik et al., 2004). Taking into consideration the role of SRC in tumors of the CNS and the potent inhibitory effect of dasatinib against SRC, dasatinib may be a promising drug for treatment of brain tumors such as GBM (Du et al., 2009; Milano et al., 2009). However, one caveat behind the use of dasatinib in CNS tumors is its ability to cross the BBB and achieve therapeutic concentrations in the brain.

Drug penetration into the CNS is often limted by active efflux proteins in the BBB, such as Pgp and BCRP. In the current study, we have shown that dasatinib is a substrate for both P-gp and BCRP using *in vitro* Pgp- and Bcrp-transfected cell models. I*n vivo* transport studies

demonstrate that these two efflux proteins significantly limit the amount of drug that traverses the BBB. Moreover, our studies have evaluated the possibility that the two drug efflux transporters act in association with each other to extrude substrate drugs out of the brain.

In a recent report, Porkka et al. suggested that dasatinib can cross the BBB to result in therapeutic response in CNS leukemia (Porkka et al., 2008). However, the group also reported that dasatinib concentrations in brain were on average 12 to 31-fold lower than in plasma. A brain penetrance of less than 10% reported in this study indicates that dasatinib does not readily cross the BBB. The group has concluded that, given the greater potency of dasatinib against BCR ABL, the CNS penetration seen was sufficient to produce antitumor activity against CML in the CNS. However, it remains to be tested that this level of CNS distribution can result in therapeutic response for other tumors of the CNS. Furthermore, considering the fact that dasatinib is being evaluated for treatment in other tumors of the brain, adequate CNS distribution of dasatinib is important. Therefore, the CNS distribution kinetics of dasatinib was evaluated *in vivo* using the FVB mouse model.

This study assessed the importance of the efflux transporters P-gp and BCRP, individually and in combination, on dasatinib brain distribution using transporter gene knockout mouse models, such as *Mdr1a/b*$^{-/-}$, *Bcrp1*$^{-/-}$ and *Mdr1a/b*$^{-/-}$ *Bcrp1*$^{-/-}$ mice. After intravenous administration in FVB wild-type mice, dasatinib demonstrated low brain penetration, with brain-to-plasma concentration ratios lower than 0.12 during the entire period of study **(Figure 4)**. This is consistent with the findings by Porkka et al. and confirms that dasatinib brain distribution is limited. In *Mdr1a/b*$^{-/-}$ *Bcrp1*$^{-/-}$ mice, this brain-to-plasma ratio increased by greater than 10-fold and reached an "equilibrium" value of 1 after one hour. This increase in the B/P ratios in the absence of P-gp and BCRP confirms the role of these two transporters in limiting brain distribution of dasatinib. To delineate the relative involvement of P-gp and BCRP in limiting dasatinib delivery across the BBB, we studied the brain concentrations in the *Mdr1a/b*$^{-/-}$ and *Bcrp1*$^{-/-}$ mice. Surprisingly, brain concentrations in the *Bcrp1*$^{-/-}$ mice were not different from those in the wild-type mice. Brain concentrations in the *Mdr1a/b*$^{-/-}$ mice were increased by greater than 6-fold (120 min) when compared to the wild-type mice **(Figure 5A)**. These findings were confirmed by the results from the pharmacological inhibition studies in FVB wild-type

JPET Fast Forward. Published on June 2, 2009 as DOI: 10.1124/jpet.109.154781
This article has not been copyedited and formatted. The final version may differ from this version.

mice. Dasatinib brain concentration in FVB wild-type mice increased 3-fold (120 min) compared to control, when they were pretreated with the P-gp selective inhibitor LY335979. However, pretreatment with the selective and potent BCRP inhibitor Ko143 was unable to result in any increase in dasatinib brain concentrations **(Figure 5B)**. One common observation from the studies in gene knockout animal group and the pharmacological inhibited animal group is that the greatest increase in brain concentration was observed when both P-gp and BCRP were knocked out or inhibited. Brain concentrations increased by greater than 18-fold in the *Mdr1a/b*$^{-/-}$ *Bcrp1*$^{-/-}$ mice **(Figure 5A)** and by greater than 10-fold in FVB wild-type mice pretreated with GF120918, the dual inhibitor of P-gp and BCRP **(Figure 5B)**. Similar results were seen on oral administration of dasatinib, the brain-to-plasma ratios increasing by 6-fold compared to control in presence of GF120918 and by over 9-fold in the *Mdr1a/b*$^{-/-}$ *Bcrp1*$^{-/-}$ mice **(Figure 6)**. These results show that while P-gp might limit the delivery of dasatinib across the BBB, BCRP alone has no such effect on dasatinib transport. Moreover, these two transporters in combination exert the highest efflux activity and brain distribution is enhanced to a significant extent when they both are pharmacologically inhibited or both are genetically deleted.

It is interesting to see that inhibition or genetic deletion of BCRP alone does not enhance brain penetration of dasatinib *in vivo*, since *in vitro* results show that dasatinib is a good BCRP substrate. One possibility could be that P-gp compensates for the loss of BCRP and is still able to extrude drugs out of the brain. Even more interesting is the dramatic increase in brain concentrations in the *Mdr1a/b*$^{-/-}$ *Bcrp1*$^{-/-}$ mice and the GF120918 pretreated FVB mice. This suggests that the two transporters work in concert in limiting delivery of dasatinib across the BBB. Remarkably, similar results have been reported for imatinib, the brain distribution increasing in absence of both P-gp and BCRP (Bihorel et al., 2007a; Bihorel et al., 2007b). In a recent study, De Vries et al. also reported such additive effect of the two transporters for topotecan, another dual substrate of P-gp and BCRP (de Vries et al., 2007). The latest report of "synergistic" activity of P-gp and BCRP in limiting CNS distribution was in a study by Polli et al. The group reported that brain-to-plasma ratio of lapatinib increased by greater than 40-fold in the Mdr1a/b$^{-/-}$ Bcrp1$^{-/-}$ mice as compared to a 4-fold increase in the Mdr1a/b$^{-/-}$ mice (Polli et al., 2009). The authors explained this greater than additive effect in the triple knockout mice by a possible "synergistic" mechanism in the action of the two transporters. The possibility of the

two efflux transporters acting synergistically at the BBB is a relatively new finding and highlights the need for future studies trying to elucidate the mechanism by which the two transporters interact with each other to limit delivery of macromolecules across the BBB. Moreover, these results demonstrate the great impact that this combinatorial action of P-gp and BCRP has on the delivery of drugs that are dual substrates to the brain.

The finding that P-gp and BCRP have a combined effect on delivery of dasatinib to the CNS has important potential consequences for the treatment of CNS metastasis in chronic myeloid leukemia and other CNS tumors. Although it was introduced to circumvent the resistance seen with imatinib therapy, dasatinib is now being evaluated for use in other tumors of the CNS. Limited CNS distribution of dasatinib may yield concentrations insufficient to adequately treat some CNS tumors, whether they are primary or secondary metastases. This could be of great importance in primary tumors of the brain like glioblastoma multiforme, where inadequate delivery of dasatinib to a highly heterogeneous tumor may significantly limit therapy. These findings also provide insight into novel therapeutic strategies, such as concurrent administration of a dual P-gp and BCRP inhibitor like elacridar, to improve brain and tumor delivery of dasatinib and other dual substrates (Breedveld et al., 2006). Similar to the reports by Polli et al. and de Vries et al., this study warrants further investigation of the possible mechanisms by which the two transporters interact with each other to limit drug delivery to the brain. The findings also highlight the need to better understand the role of BCRP at the blood-brain barrier.

In summary, dasatinib is a substrate of efflux transporters P-gp and BCRP and these two transport proteins play a central role in limiting CNS delivery of dasatinib. The use of potent inhibitors of both P-gp and BCRP should be able to improve CNS delivery and may provide a potential therapeutic strategy to improve delivery and efficacy of dasatinib against CNS tumors. This finding will have direct clinical implications in the treatment of primary and metastatic brain tumors with dasatinib and is one mechanism that may be exploited to improve delivery across the blood-brain barrier and the tumor cell barrier.

References

(2006) Dasatinib: BMS 354825. *Drugs R D* **7**:129-132.

Allen JD, van Loevezijn A, Lakhai JM, van der Valk M, van Tellingen O, Reid G, Schellens JH, Koomen GJ, Schinkel AH (2002) Potent and specific inhibition of the breast cancer resistance protein multidrug transporter in vitro and in mouse intestine by a novel analogue of fumitremorgin C. *Molecular Cancer Therapeutics* **1**:417-425.

Bihorel S, Camenisch G, Lemaire M and Scherrmann JM (2007a) Influence of breast cancer resistance protein (Abcg2) and p-glycoprotein (Abcb1a) on the transport of imatinib mesylate (Gleevec) across the mouse blood-brain barrier. *J Neurochem* **102**:1749-1757.

Bihorel S, Camenisch G, Lemaire M and Scherrmann JM (2007b) Modulation of the brain distribution of imatinib and its metabolites in mice by valspodar, zosuquidar and elacridar. *Pharm Res* **24**:1720-1728.

Breedveld P, Beijnen JH and Schellens JH (2006) Use of P-glycoprotein and BCRP inhibitors to improve oral bioavailability and CNS penetration of anticancer drugs. *Trends Pharmacol Sci* **27**:17-24.

Breedveld P, Pluim D, Cipriani G, Wielinga P, van Tellingen O, Schinkel AH and Schellens JH (2005) The effect of Bcrp1 (Abcg2) on the in vivo pharmacokinetics and brain penetration of imatinib mesylate (Gleevec): implications for the use of breast cancer resistance protein and P-glycoprotein inhibitors to enable the brain penetration of imatinib in patients. *Cancer Res* **65**:2577-2582.

Cortes J, Rousselot P, Kim DW, Ritchie E, Hamerschlak N, Coutre S, Hochhaus A, Guilhot F, Saglio G, Apperley J, Ottmann O, Shah N, Erben P, Branford S, Agarwal P, Gollerkeri A and Baccarani M (2007) Dasatinib induces complete hematologic and cytogenetic

responses in patients with imatinib-resistant or -intolerant chronic myeloid leukemia in blast crisis. *Blood* **109**:3207-3213.

Dai H, Marbach P, Lemaire M, Hayes M and Elmquist WF (2003) Distribution of STI-571 to the brain is limited by P-glycoprotein-mediated efflux. *Journal of Pharmacology & Experimental Therapeutics* **304**:1085-1092.

Dai Y, Rahmani M, Corey SJ, Dent P and Grant S (2004) A Bcr/Abl-independent, Lyn-dependent form of imatinib mesylate (STI-571) resistance is associated with altered expression of Bcl-2. *J Biol Chem* **279**:34227-34239.

de Vries NA, Zhao J, Kroon E, Buckle T, Beijnen JH and van Tellingen O (2007) P-glycoprotein and breast cancer resistance protein: two dominant transporters working together in limiting the brain penetration of topotecan. *Clin Cancer Res* **13**:6440-6449.

Donato NJ, Wu JY, Stapley J, Gallick G, Lin H, Arlinghaus R and Talpaz M (2003) BCR-ABL independence and LYN kinase overexpression in chronic myelogenous leukemia cells selected for resistance to STI571. *Blood* **101**:690-698.

Druker BJ (2003a) David A. Karnofsky Award lecture. Imatinib as a paradigm of targeted therapies. *Journal of Clinical Oncology* **21**:239s-245s.

Druker BJ (2003b) Overcoming resistance to imatinib by combining targeted agents. *Mol Cancer Ther* **2**:225-226.

Du J, Bernasconi P, Clauser KR, Mani DR, Finn SP, Beroukhim R, Burns M, Julian B, Peng XP, Hieronymus H, Maglathlin RL, Lewis TA, Liau LM, Nghiemphu P, Mellinghoff IK, Louis DN, Loda M, Carr SA, Kung AL and Golub TR (2009) Bead-based profiling of tyrosine kinase phosphorylation identifies SRC as a potential target for glioblastoma therapy. *Nat Biotechnol* **27**:77-83.

Kantarjian H, Pasquini R, Hamerschlak N, Rousselot P, Holowiecki J, Jootar S, Robak T, Khoroshko N, Masszi T, Skotnicki A, Hellmann A, Zaritsky A, Golenkov A, Radich J, Hughes T, Countouriotis A and Shah N (2007) Dasatinib or high-dose imatinib for chronic-phase chronic myeloid leukemia after failure of first-line imatinib: a randomized phase 2 trial. *Blood* **109**:5143-5150.

Leis JF, Stepan DE, Curtin PT, Ford JM, Peng B, Schubach S, Druker BJ and Maziarz RT (2004) Central nervous system failure in patients with chronic myelogenous leukemia lymphoid blast crisis and Philadelphia chromosome positive acute lymphoblastic leukemia treated with imatinib (STI-571). *Leukemia & Lymphoma* **45**:695-698.

Lombardo LJ, Lee FY, Chen P, Norris D, Barrish JC, Behnia K, Castaneda S, Cornelius LA, Das J, Doweyko AM, Fairchild C, Hunt JT, Inigo I, Johnston K, Kamath A, Kan D, Klei H, Marathe P, Pang S, Peterson R, Pitt S, Schieven GL, Schmidt RJ, Tokarski J, Wen ML, Wityak J and Borzilleri RM (2004) Discovery of N-(2-chloro-6-methyl- phenyl)-2-(6-(4-(2-hydroxyethyl)- piperazin-1-yl)-2-methylpyrimidin-4- ylamino)thiazole-5-carboxamide (BMS-354825), a dual Src/Abl kinase inhibitor with potent antitumor activity in preclinical assays. *J Med Chem* **47**:6658-6661.

Milano V, Piao Y, Lafortune T and de Groot J (2009) Dasatinib-induced autophagy is enhanced in combination with temozolomide in glioma. *Mol Cancer Ther* **8**:394-406.

Nam S, Kim D, Cheng JQ, Zhang S, Lee JH, Buettner R, Mirosevich J, Lee FY and Jove R (2005) Action of the Src family kinase inhibitor, dasatinib (BMS-354825), on human prostate cancer cells. *Cancer Res* **65**:9185-9189.

Neville K, Parise RA, Thompson P, Aleksic A, Egorin MJ, Balis FM, McGuffey L, McCully C, Berg SL and Blaney SM (2004) Plasma and cerebrospinal fluid pharmacokinetics of

imatinib after administration to nonhuman primates. *Clinical Cancer Research* **10**:2525-2529.

Ottmann O, Dombret H, Martinelli G, Simonsson B, Guilhot F, Larson RA, Rege-Cambrin G, Radich J, Hochhaus A, Apanovitch AM, Gollerkeri A and Coutre S (2007) Dasatinib induces rapid hematologic and cytogenetic responses in adult patients with Philadelphia chromosome positive acute lymphoblastic leukemia with resistance or intolerance to imatinib: interim results of a phase 2 study. *Blood* **110**:2309-2315.

Ottmann OG, Druker BJ, Sawyers CL, Goldman JM, Reiffers J, Silver RT, Tura S, Fischer T, Deininger MW, Schiffer CA, Baccarani M, Gratwohl A, Hochhaus A, Hoelzer D, Fernandes-Reese S, Gathmann I, Capdeville R and O'Brien SG (2002) A phase 2 study of imatinib in patients with relapsed or refractory Philadelphia chromosome-positive acute

Polli JW, Olson KL, Chism JP, John-Williams LS, Yeager RL, Woodard SM, Otto V, Castellino S and Demby VE (2009) An unexpected synergist role of P-glycoprotein and breast cancer resistance protein on the central nervous system penetration of the tyrosine kinase inhibitor lapatinib (N-{3-chloro-4-[(3-fluorobenzyl)oxy]phenyl}-6-[5-({[2-(methylsulfonyl)ethy l]amino}methyl)-2-furyl]-4-quinazolinamine; GW572016). *Drug Metab Dispos* **37**:439-442.

Porkka K, Koskenvesa P, Lundan T, Rimpilainen J, Mustjoki S, Smykla R, Wild R, Luo R, Arnan M, Brethon B, Eccersley L, Hjorth-Hansen H, Hoglund M, Klamova H, Knutsen H, Parikh S, Raffoux E, Gruber F, Brito-Babapulle F, Dombret H, Duarte RF, Elonen E, Paquette R, Zwaan CM and Lee FY (2008) Dasatinib crosses the blood-brain barrier and is an efficient therapy for central nervous system Philadelphia chromosome-positive leukemia. *Blood* **112**:1005-1012.

Ptasznik A, Nakata Y, Kalota A, Emerson SG and Gewirtz AM (2004) Short interfering RNA (siRNA) targeting the Lyn kinase induces apoptosis in primary, and drug-resistant, BCR-ABL1(+) leukemia cells. *Nat Med* **10**:1187-1189.

Quintas-Cardama A, Kantarjian H and Cortes J (2007) Flying under the radar: the new wave of BCR-ABL inhibitors. *Nat Rev Drug Discov* **6**:834-848.

Rajappa S, Uppin SG, Raghunadharao D, Rao IS and Surath A (2004) Isolated central nervous system blast crisis in chronic myeloid leukemia. *Hematological Oncology* **22**:179-181.

Sawyers CL, Hochhaus A, Feldman E, Goldman JM, Miller CB, Ottmann OG, Schiffer CA, Talpaz M, Guilhot F, Deininger MW, Fischer T, O'Brien SG, Stone RM, Gambacorti-Passerini CB, Russell NH, Reiffers JJ, Shea TC, Chapuis B, Coutre S, Tura S, Morra E, Larson RA, Saven A, Peschel C, Gratwohl A, Mandelli F, Ben-Am M, Gathmann I, Capdeville R, Paquette RL and Druker BJ (2002) Imatinib induces hematologic and cytogenetic responses in patients with chronic myelogenous leukemia in myeloid blast crisis: results of a phase II study. *Blood* **99**:3530-3539.

Shah NP (2007) Medical Management of CML. *Hematology Am Soc Hematol Educ Program* **2007**:371-375.

Footnotes

This work was supported by a grant from the Leukemia Research Fund to the University of Minnesota.

This work was originally presented at the 15th North American Regional ISSX Meeting, October 2008. Drug Metab Rev. 2008; 40 Suppl 3:1-308.

Reprint Requests:
William F. Elmquist, Department of Pharmaceutics, University of Minnesota, 9-177 Weaver Densford Hall, 308 Harvard Street SE, Minneapolis, MN 55455, USA. Phone: +001-612-625-0097; Fax: +001-612-626-2125; e-mail: elmqu011@umn.edu

JPET Fast Forward. Published on June 2, 2009 as DOI: 10.1124/jpet.109.154781
This article has not been copyedited and formatted. The final version may differ from this version.

Legends for Figures:

Figure 1. Accumulation of [^{14}C] dasatinib and [^{3}H] vinblastine (positive control) in wild-type (black bar) and MDR1-transfected (gray bar) MDCKII cells and the effect of P-gp inhibitor LY335979 (1µM). Results are presented as mean ±S.D. (as percentage of wild-type control), *n* =4 to 12. (**, p<0.01 compared to wild-type control, ††, p<0.01 compared to treatment control). Vinblastine was used as positive control for P-gp function. Treatment with LY335979 restored dasatinib accumulation in the MDR1 cells such that it was not different than wild-type control.

Figure 2. Accumulation of [^{14}C] dasatinib and [^{3}H] mitoxantrone (positive control) in wild-type (black bar) and Bcrp1-transfected (gray bar) MDCKII cells and the effect of BCRP inhibitor Ko143 (200nM). Results are expressed as mean ±S.D. (as percentage of wild-type control), *n* =6 to 12. (**, p<0.01 compared to wild-type control, ††, p<0.01 compared to treatment control). Mitoxantrone was used as positive control for BCRP function. Treatment with Ko143 restored dasatinib accumulation in the Bcrp1-transfected cells such that it was not different than wild-type control.

Figure 3. Brain distribution of dasatinib in wild-type and Mdr1a/b$^{(-/-)}$Bcrp1$^{(-/-)}$ FVB Mice after an intravenous dose of 5 mg/kg dasatinib via tail vein injection. Plasma and whole brain tissue were collected at 5, 20, 60, 120 and 180 minutes postdose (n=4 at each time point) and analyzed by LC-MS/MS. Dasatinib concentration-time profiles in plasma **(A)** and brain **(B)** in wild-type **(●)** and Mdr1a/b$^{(-/-)}$Bcrp1$^{(-/-)}$ **(▲)** FVB mice. Brain concentrations in the Mdr1a/b$^{(-/-}$

JPET Fast Forward. Published on June 2, 2009 as DOI: 10.1124/jpet.109.154781
This article has not been copyedited and formatted. The final version may differ from this version.

)Bcrp1$^{(-/-)}$ were significantly greater than the wild-type at all time points. Results are represented as mean ± SE. (* p<0.001 compared to wild-type control).

Figure 4. Comparison of brain-to-plasma concentration ratios (Cb/Cp) between wild-type (●) and Mdr1a/b$^{(-/-)}$Bcrp1$^{(-/-)}$(▲) FVB mice. Cb/Cp ratios for dasatinib in the Mdr1a/b$^{(-/-}$)Bcrp1$^{(-/-)}$ were significantly greater than the Cb/Cp ratios in wild-type at all time points. Results are represented as mean ± SE. (* p<0.001 compared to wild-type control).

Figure 5. (A) Effect of pharmacological inhibition of drug efflux transporters on brain distribution of dasatinib in wild-type FVB mice. Wild-type mice received 5mg/kg dasatinib via tail vein injection 30 minutes after i.v. administration of 25 mg/kg LY335979, 10 mg/kg Ko143 or 10 mg/kg GF120918. **(B) Effect of genetic deletion of drug efflux transporters on brain distribution of dasatinib in FVB mice.** Wild-type, *Mdr1a/b*$^{-/-}$, *Bcrp1*$^{-/-}$, *Mdr1a/b*$^{-/-}$ *Bcrp1*$^{-/-}$ mice were administered 5 mg/kg dasatinib via tail vein injection. Whole brain tissue were collected at 20 and 120 minutes postdose (n=4 at each time point) and analyzed for dasatinib. The values are presented as mean ± S.E. (** p<0.001, compared to wild-type control, †† p<0.05, compared to wild-type control).

Figure 6. Effect of pharmacological inhibition and genetic deletion of drug efflux transporters on brain-to-plasma distribution ratio of dasatinib after an oral dose in FVB mice. Wild-type mice were administered an oral dose of 10 mg/kg dasatinib 30 minutes after i.v. administration of 25 mg/kg LY335979, 10 mg/kg Ko143 or 10 mg/kg GF120918. For the genetic deletion study, wild-type, *Mdr1a/b*$^{-/-}$, *Bcrp1*$^{-/-}$, *Mdr1a/b*$^{-/-}$ *Bcrp1*$^{-/-}$ mice were

administered a 10 mg/kg oral dose of dasatinib. Plasma and brain were collected at 120 minutes postdose (n=4 at each time point). Similar to the i.v. study, the brain-to-plasma ratio increased when P-gp was inhibited or genetically deleted. While absence of BCRP did not cause any change, the greatest change in brain distribution was seen when both P-gp and BCRP was inhibited or absent. The values are presented as mean ± S.E. (** $p<0.01$, compared to wild-type control).

JPET Fast Forward. Published on June 2, 2009 as DOI: 10.1124/jpet.109.154781
This article has not been copyedited and formatted. The final version may differ from this version.

Table 1A. Effective permeabilities (P_{eff}) and efflux ratios (ER) of [^{14}C] dasatinib across wild-type and MDR1-transfected MDCKII cell monolayers, in presence and absence of P-gp inhibitor LY335979 (1 µM).

	MDCK wild-type (control)			MDCK MDR1- transfected		
	A-to-B P_{eff}	B-to-A P_{eff}	ER	A-to-B P_{eff}	B-to-A P_{eff}	ER
	(Mean ± SD) x 10^{-6} *cm/s*			(Mean ± SD) x 10^{-6} *cm/s*		
Treatment control	2.02 ± 0.33	9.64 ± 0.98*	4.8	0.45 ± 0.05	11.58 ± 0.65*	25.6
1 µM LY335979	5.16 ± 0.15†	4.83 ± 0.19†	0.9	3.79 ± 0.37†	4.53 ± 0.10†	1.2

* p<0.001 compared to A-to-B, † p<0.001 compared to treatment control

JPET Fast Forward. Published on June 2, 2009 as DOI: 10.1124/jpet.109.154781
This article has not been copyedited and formatted. The final version may differ from this version.

Table 1B. Effective permeabilities (P_{eff}) and efflux ratios (ER) of [^{14}C] dasatinib across wild-type and Bcrp1-transfected MDCKII cell monolayers, in presence and absence of BCRP inhibitor Ko143 (200 nM).

	MDCK wild-type (control)			MDCK Bcrp1- transfected		
	A-to-B P_{eff}	B-to-A P_{eff}	ER	A-to-B P_{eff}	B-to-A P_{eff}	ER
	(Mean ± SD) x 10^{-6} *cm/s*			(Mean ± SD) x 10^{-6} *cm/s*		
Treatment control	3.09 ± 0.61	12.73 ± 0.60*	4.1	0.31 ± 0.25	16.20 ± 0.66*	51.6
200 nM Ko143	2.60 ± 0.10	10.68 ± 0.63*	4.1	1.66 ± 0.10†	15.19 ± 0.56*	9.2

* p<0.001 compared to A-to-B transport, † p<0.001 compared to treatment control

`

JPET Fast Forward. Published on June 2, 2009 as DOI: 10.1124/jpet.109.154781
This article has not been copyedited and formatted. The final version may differ from this version.

Figure 1

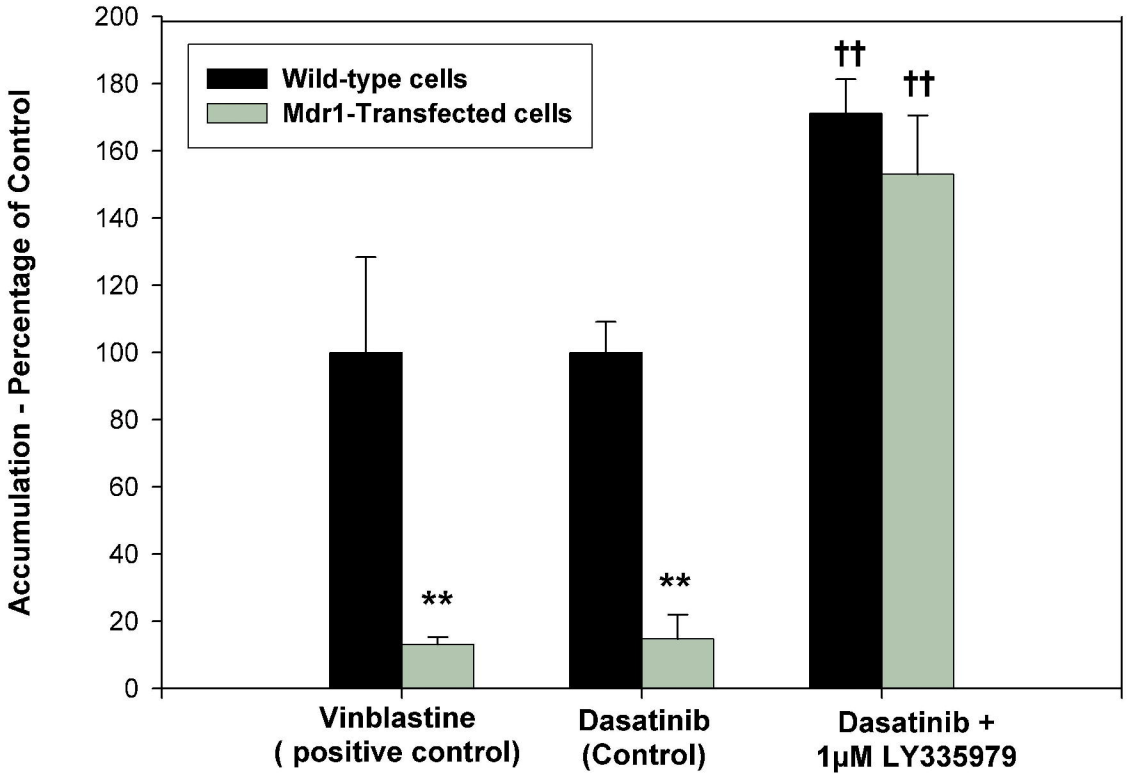

JPET Fast Forward. Published on June 2, 2009 as DOI: 10.1124/jpet.109.154781
This article has not been copyedited and formatted. The final version may differ from this version.

Figure 2

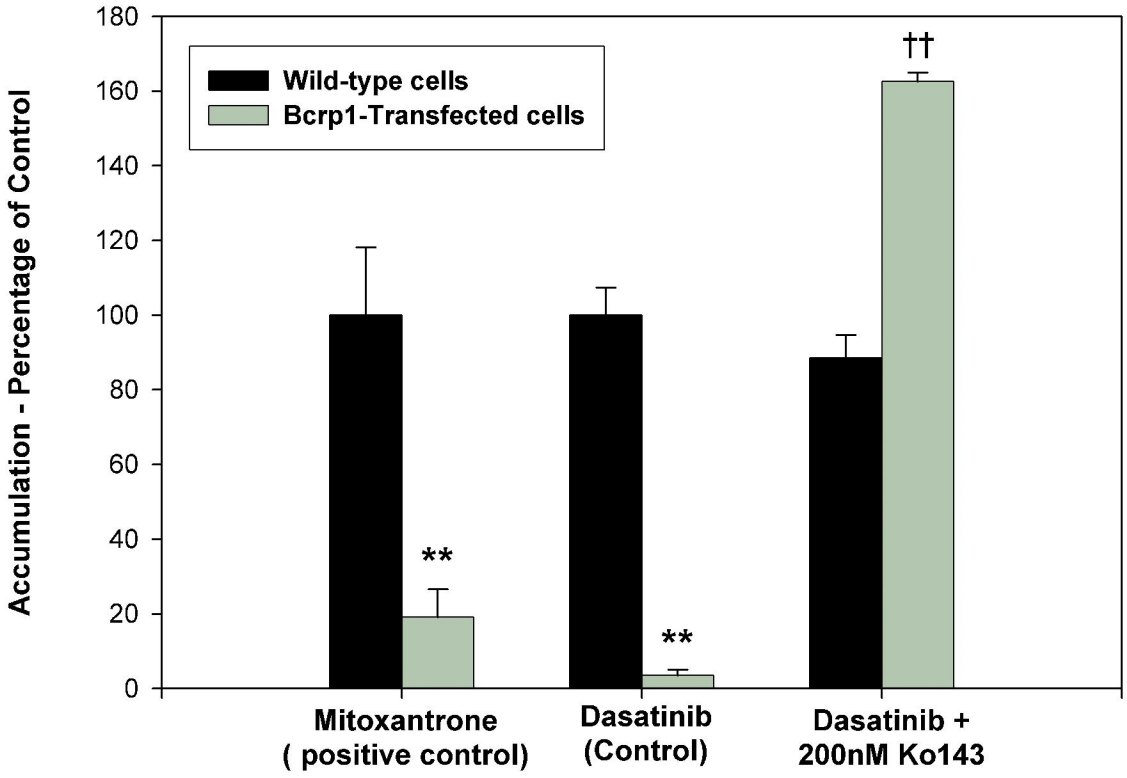

JPET Fast Forward. Published on June 2, 2009 as DOI: 10.1124/jpet.109.154781
This article has not been copyedited and formatted. The final version may differ from this version.

Figure 3A

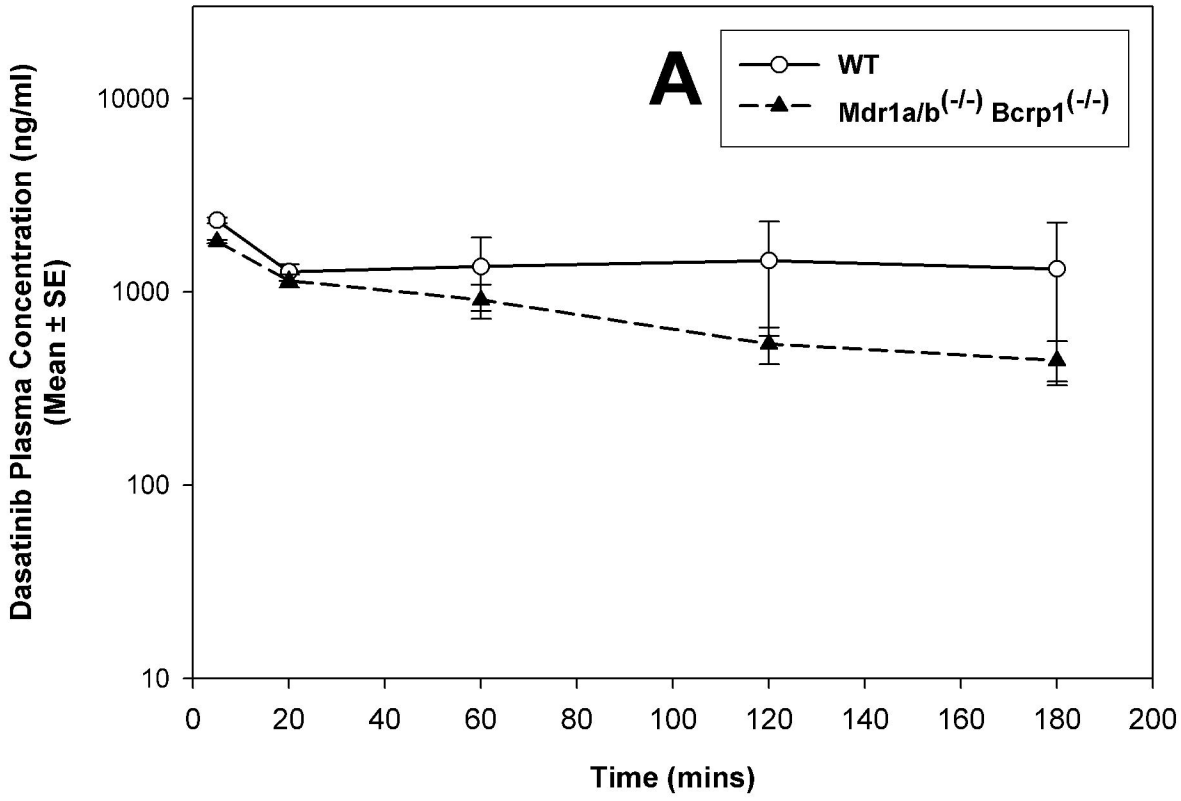

JPET Fast Forward. Published on June 2, 2009 as DOI: 10.1124/jpet.109.154781
This article has not been copyedited and formatted. The final version may differ from this version.

Figure 3B

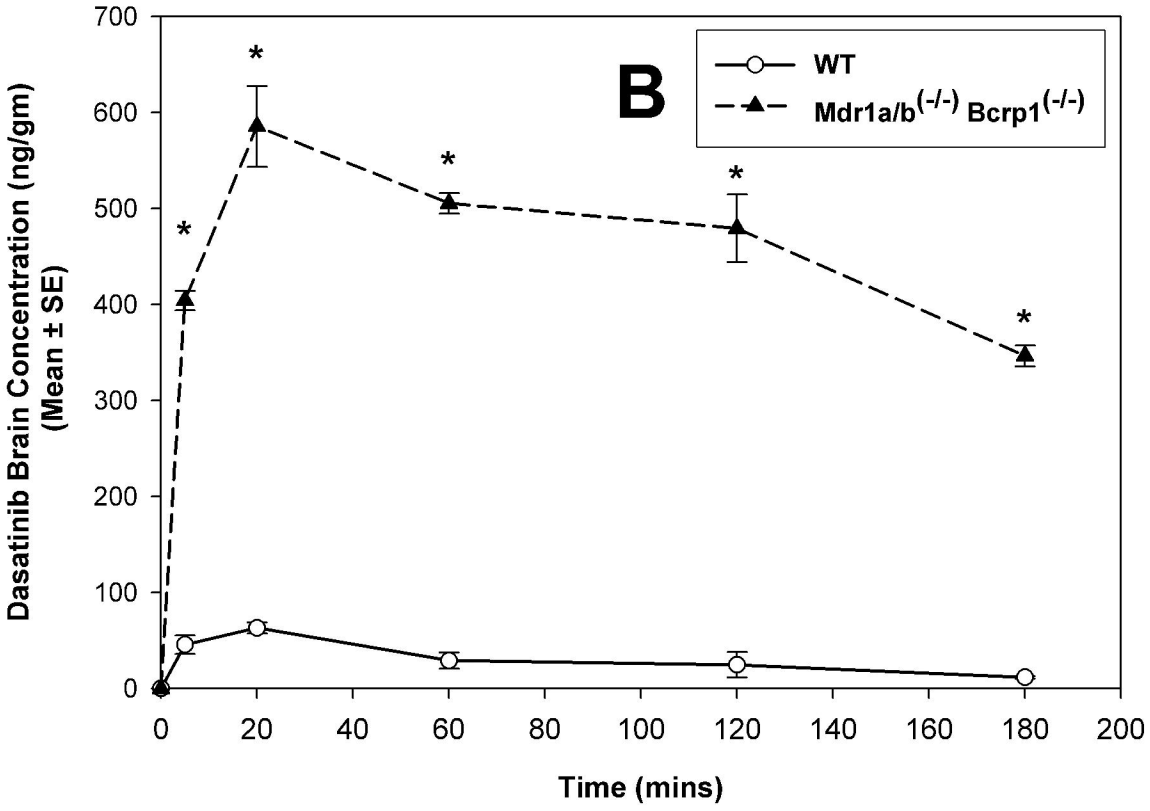

JPET Fast Forward. Published on June 2, 2009 as DOI: 10.1124/jpet.109.154781

Figure 4

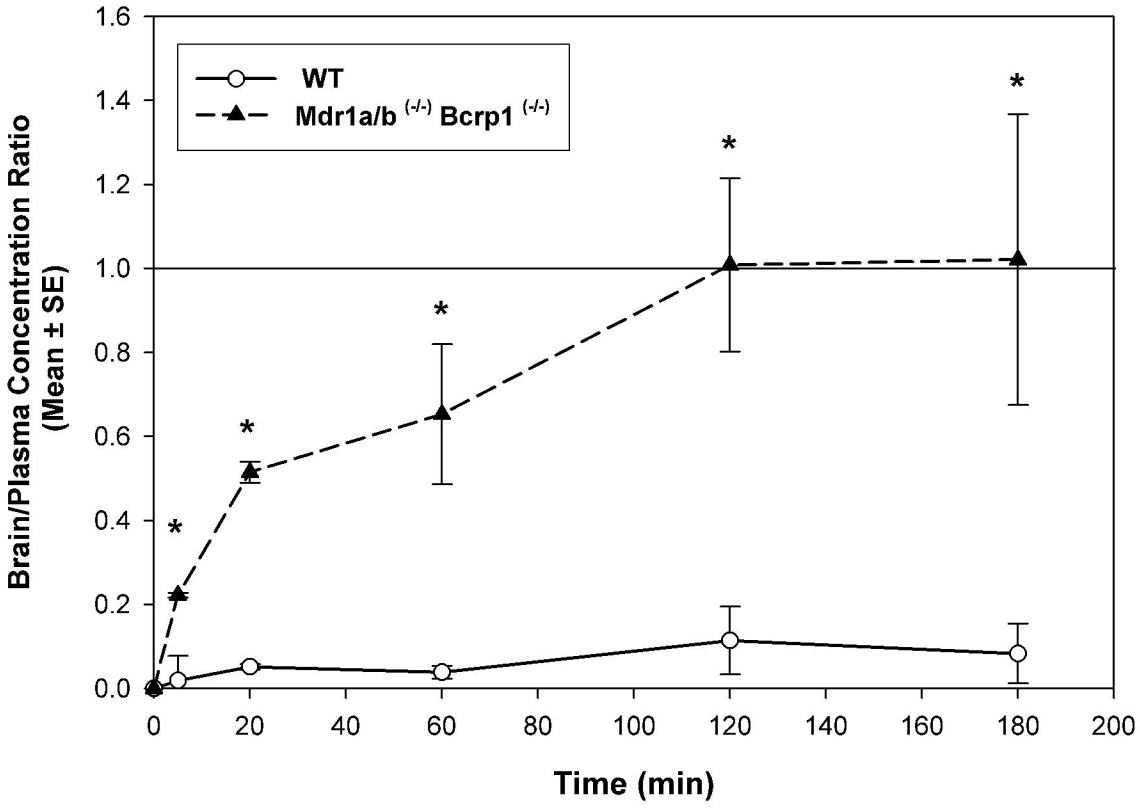

JPET Fast Forward. Published on June 2, 2009 as DOI: 10.1124/jpet.109.154781
This article has not been copyedited and formatted. The final version may differ from this version.

Figure 5A

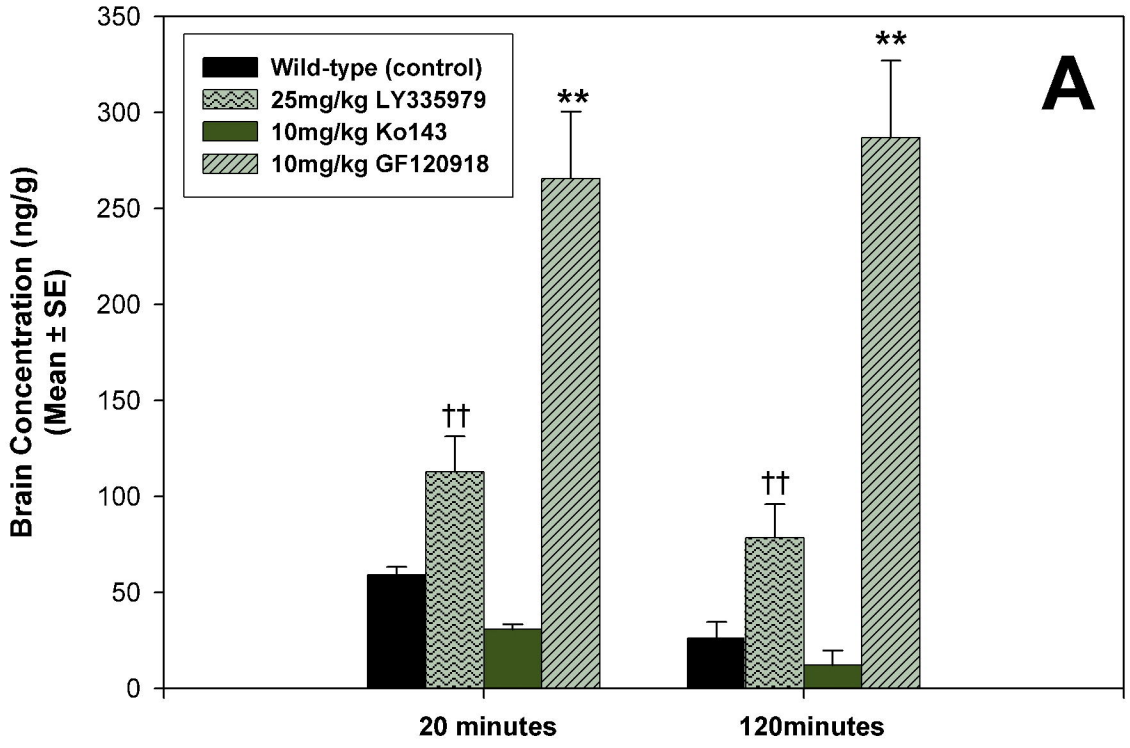

JPET Fast Forward. Published on June 2, 2009 as DOI: 10.1124/jpet.109.154781
This article has not been copyedited and formatted. The final version may differ from this version.

Figure 5B

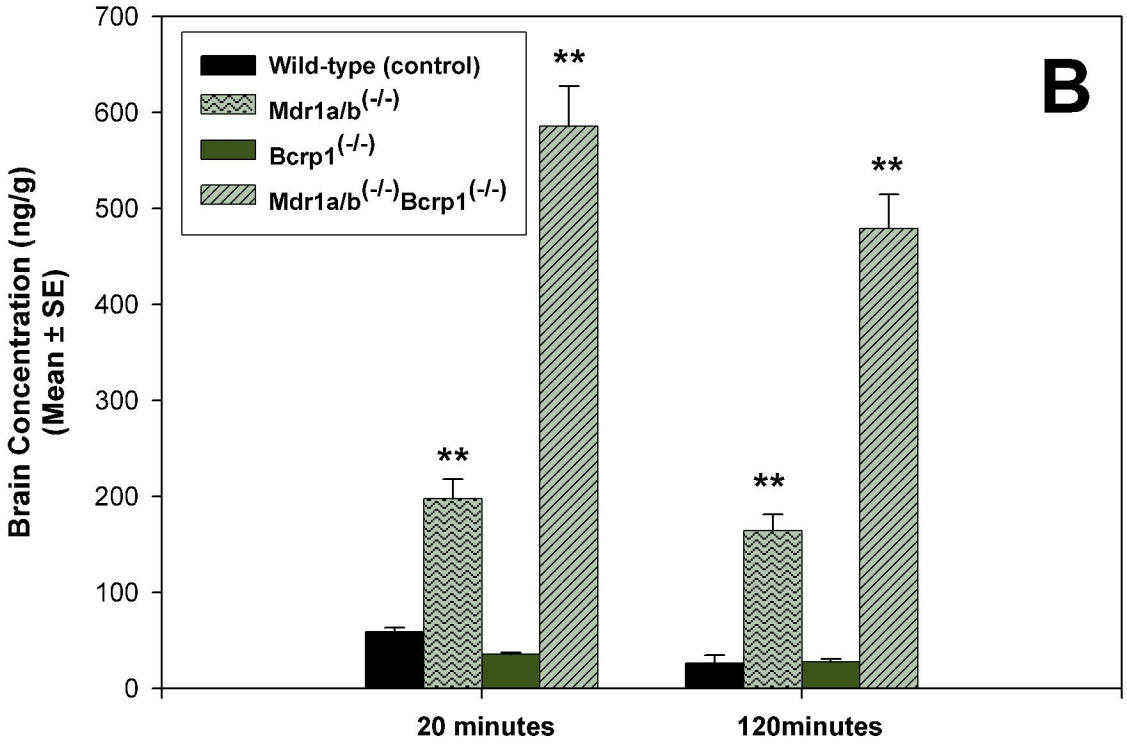

JPET Fast Forward. Published on June 2, 2009 as DOI: 10.1124/jpet.109.154781
This article has not been copyedited and formatted. The final version may differ from this version.

Figure 6